

Supplementary Information

Implementation of Reconfigurable Logic-In Memory in a Cultured Neuronal Network with a Crossbar Structure

Yonghee Bae,^a Kyo-Seok Lee,^a Sun-Mi Lee,^b Jeong-O Lee,^c Kyung-Hwa Yoo^{*ab}

^a Department of Physics, Yonsei University, Seoul 03722, Republic of Korea

^b Nanomedical Graduate Program, Yonsei University, Seoul 03722, Republic of Korea

^c Advanced Materials Division, Korea Research Institute of Chemical Technology, Daejeon 34114, Republic of
Korea

* Corresponding author, *E-mail address*: khyoo@yonsei.ac.kr

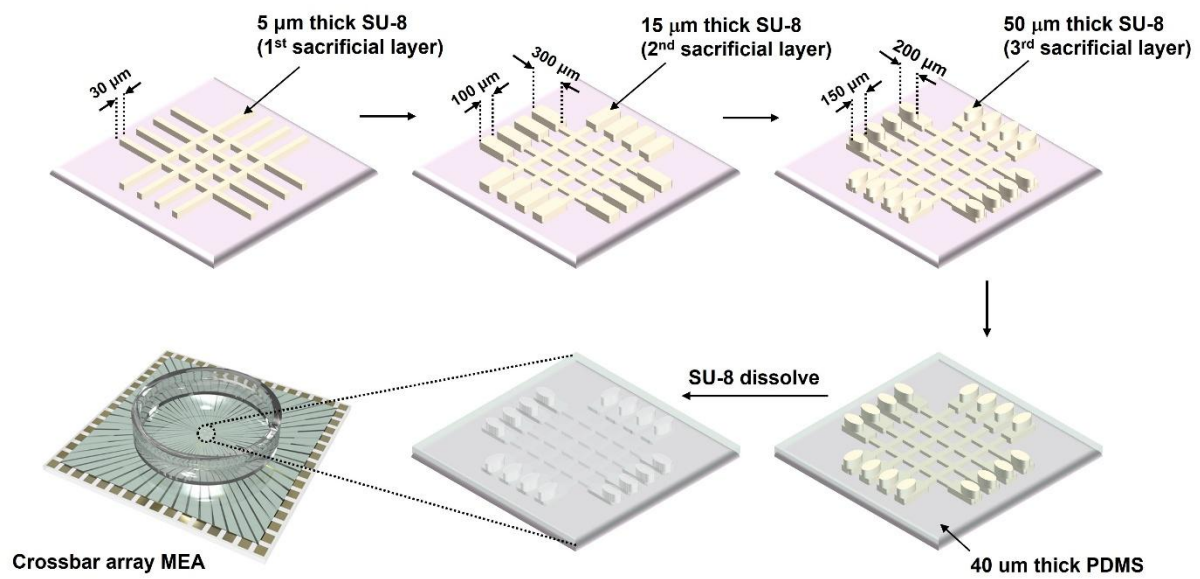


Fig. S1 Fabrication procedure for the PDMS microstructure on the MEA.

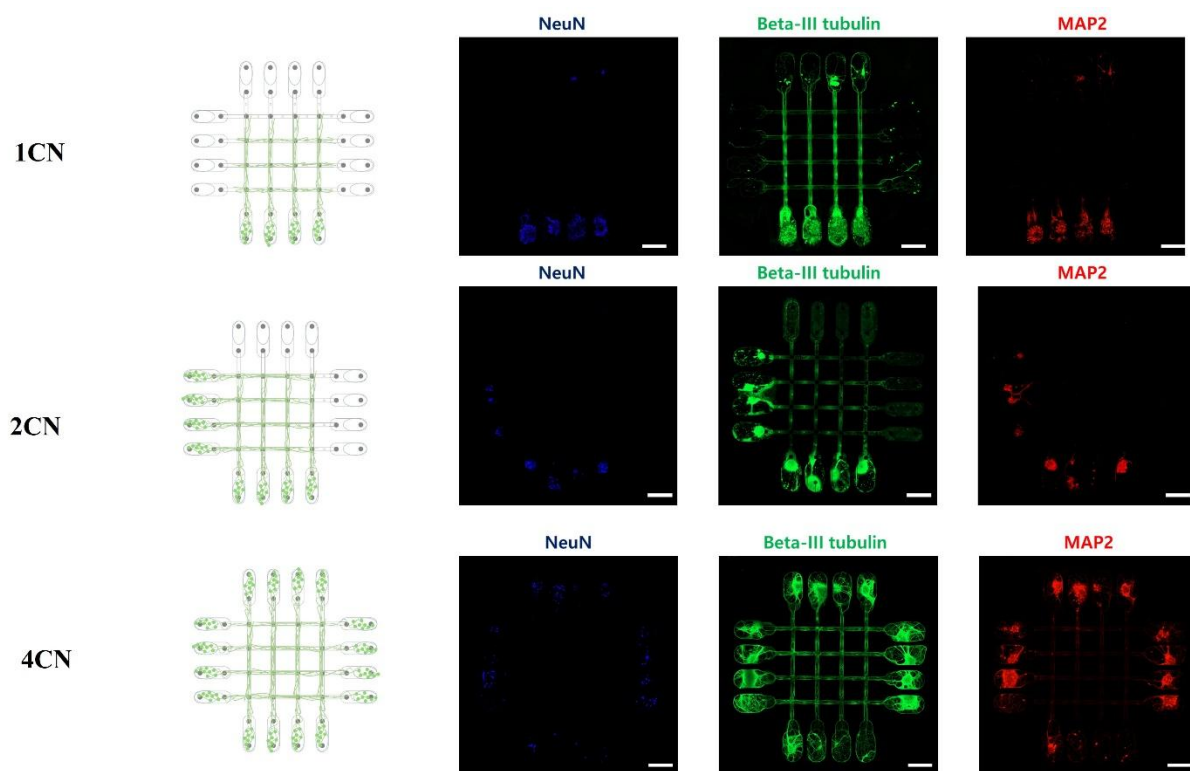
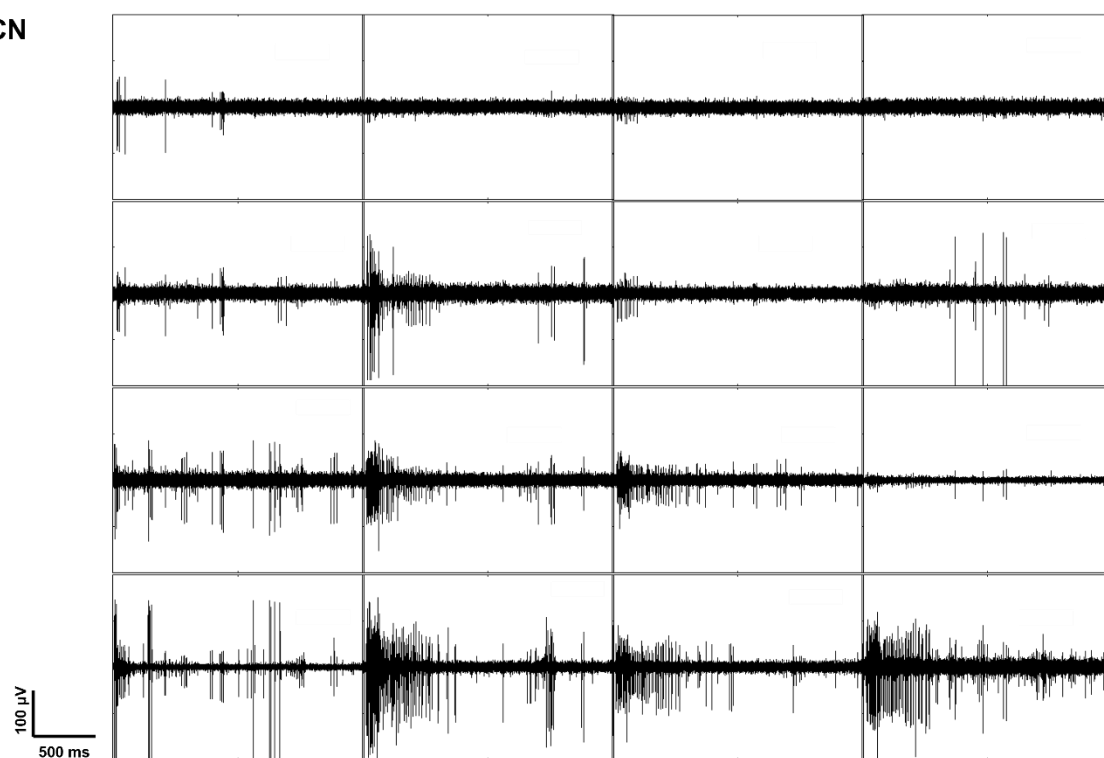
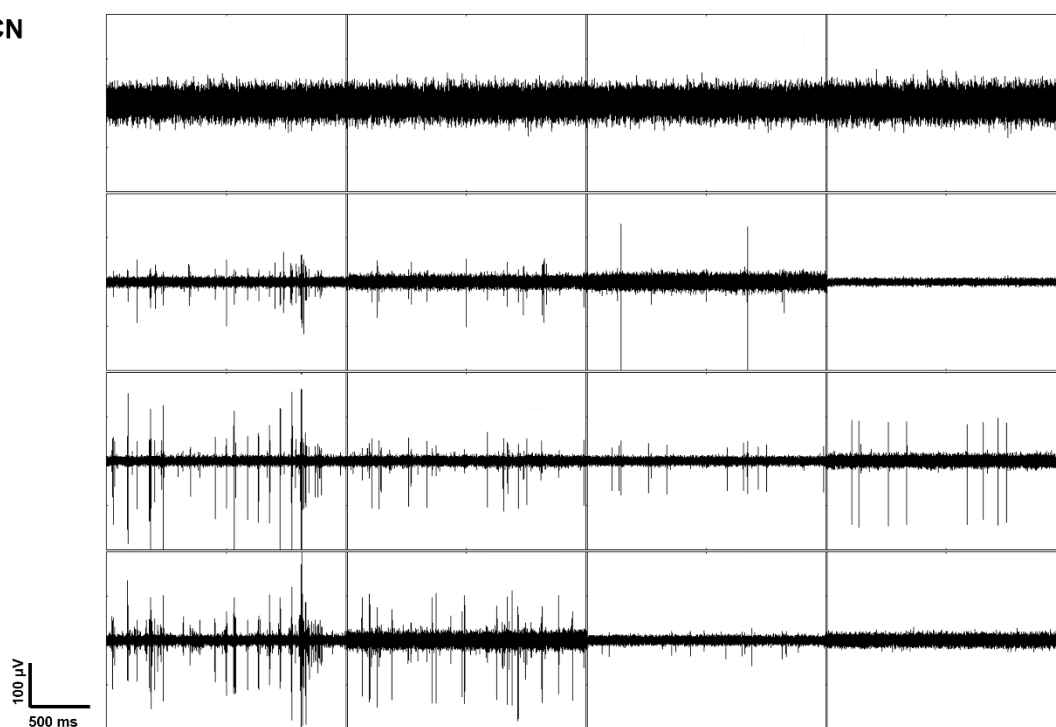


Fig. S2 Schematic of three types of neural networks: 1CN, 2CN, and 4CN. Immunofluorescence images of neural networks stained with NeuN (nuclei, blue), β -tubulin III (axons, green), and MAP2 (dendrites, red). Scale bar represents 200 μ m.

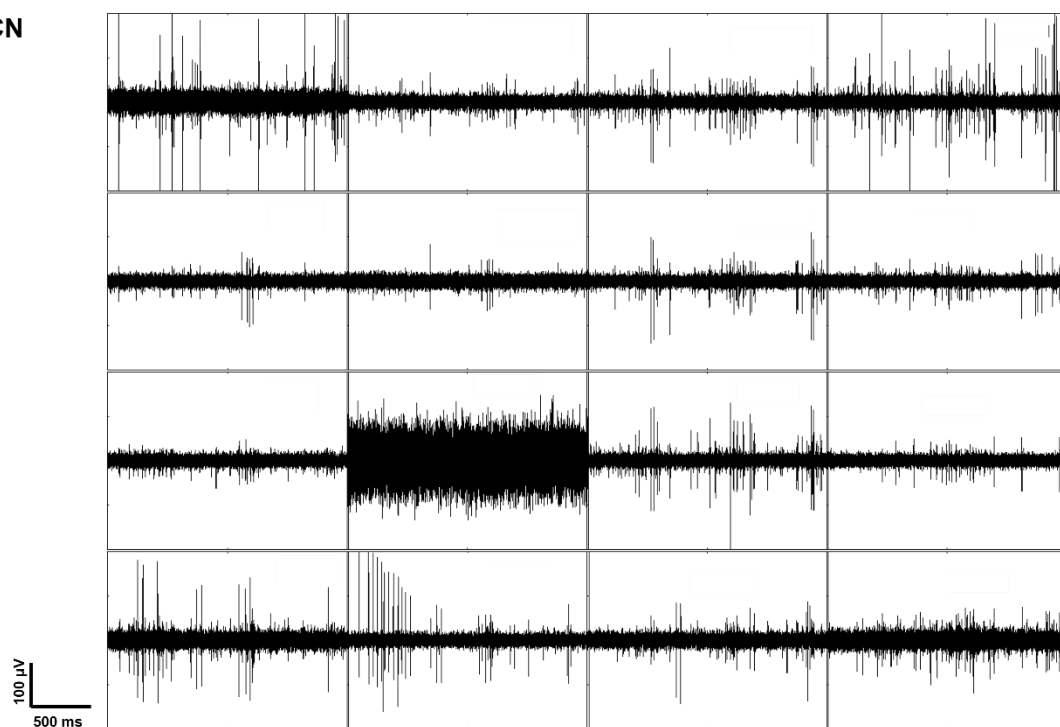
(a) 1CN



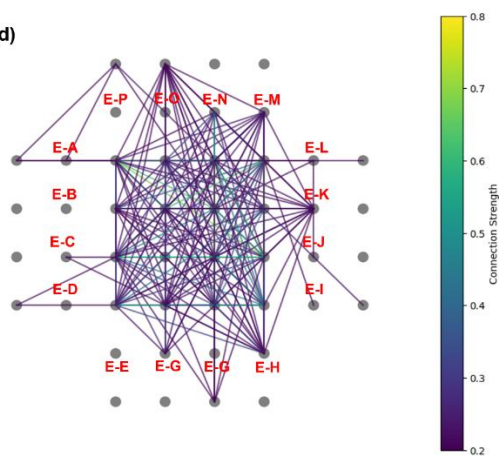
(b) 2CN



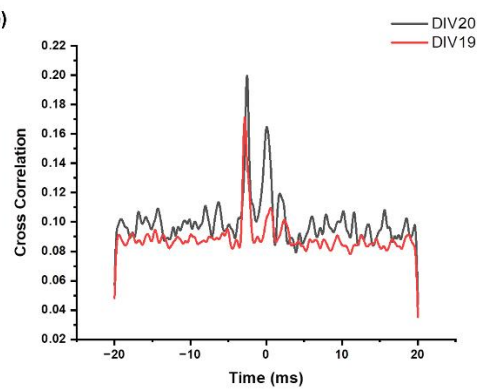
(c) 4CN



(d)



(e)



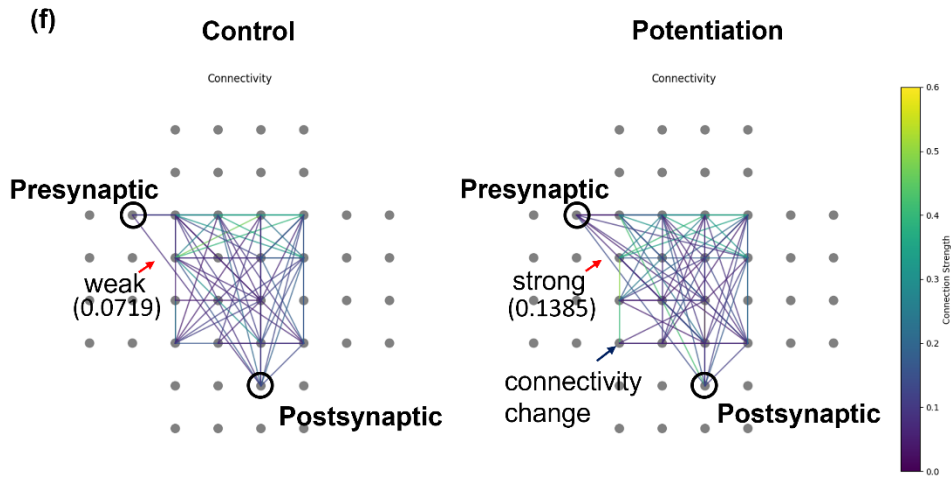


Fig. S3 Spontaneous neuronal activities recorded from channel electrodes with (a) 1CN, (b) 2CN, and (c) 4CN. The signals acquired from electrodes in the chambers (E-A ~ E-P) were significantly smaller compared to those recorded using electrodes in the channels (E11~E44), as reported by others¹⁻³. Therefore, only signals recorded using E11~E44 are shown. (d) Cross-correlation-based functional connectivity derived from spontaneous data. (e) Cross correlation between E-M and E-H used as presynaptic and postsynaptic neurons before and after STDP learning. DIV 19 and DIV 20 indicate before and after STDP learning, respectively. (f) Cross-correlation-based functional connectivity derived from spontaneous data recorded before (control) and immediately after potentiation. The connectivity between the presynaptic and postsynaptic electrodes increased from 0.0719 to 0.1385.

References

- 1 R. Habibey, S. Latifi, H. Mousavi, M. Pesce, E. Arab- and A. Blau, *Sci. Rep.*, **7** 2017, 1–14.
- 2 N. Hong, S. Joo and Y. Nam, *IEEE Trans. Biomed. Eng.*, 2017, **64**, 492–498.
- 3 A. Pelkonen, R. Mzezewa, L. Sukki, T. Ryyänen, J. Kreutzer, T. Hyvärinen, A. Vinogradov, L. Aarnos, J. Lekkala, P. Kallio and S. Narkilahti, *Biosens. Bioelectron.*, 2020, **168**, 112553.

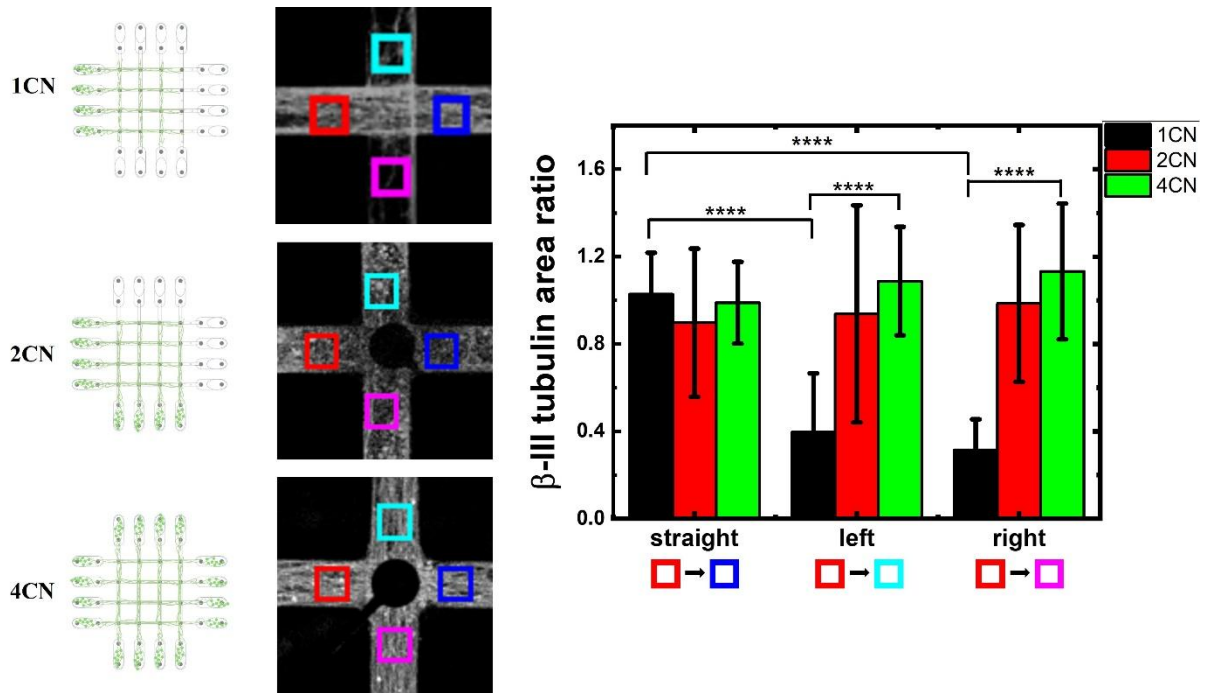


Fig. S4 Comparison of axonal directionality in crossbar neuron network with 1CN, 2CN, and 4CN. The three fluorescent images show the β -tubulin III-stained data of 1CN, 2CN and 4CN. Based on the red square region, the axon ratio in the blue box region is classified as "straight", in the cyan box region as "left", and in the magenta box region as "right". The data are presented in the plots as mean \pm standard deviations of the mean ($n = 16$). **** $p < 0.0001$, Welch's t-test.

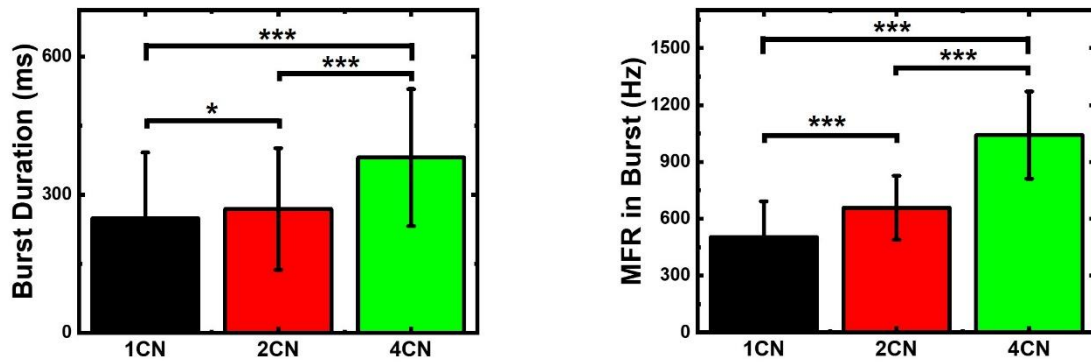


Fig. S5 Burst duration and mean firing rate (MFR) in a burst estimated from the spontaneous electrical activities of 1CN, 2CN and 4CN. The data are presented in the plots as mean \pm standard deviation ($n > 24$). * $p < 0.05$, *** $p < 0.001$, Welch's t-test.

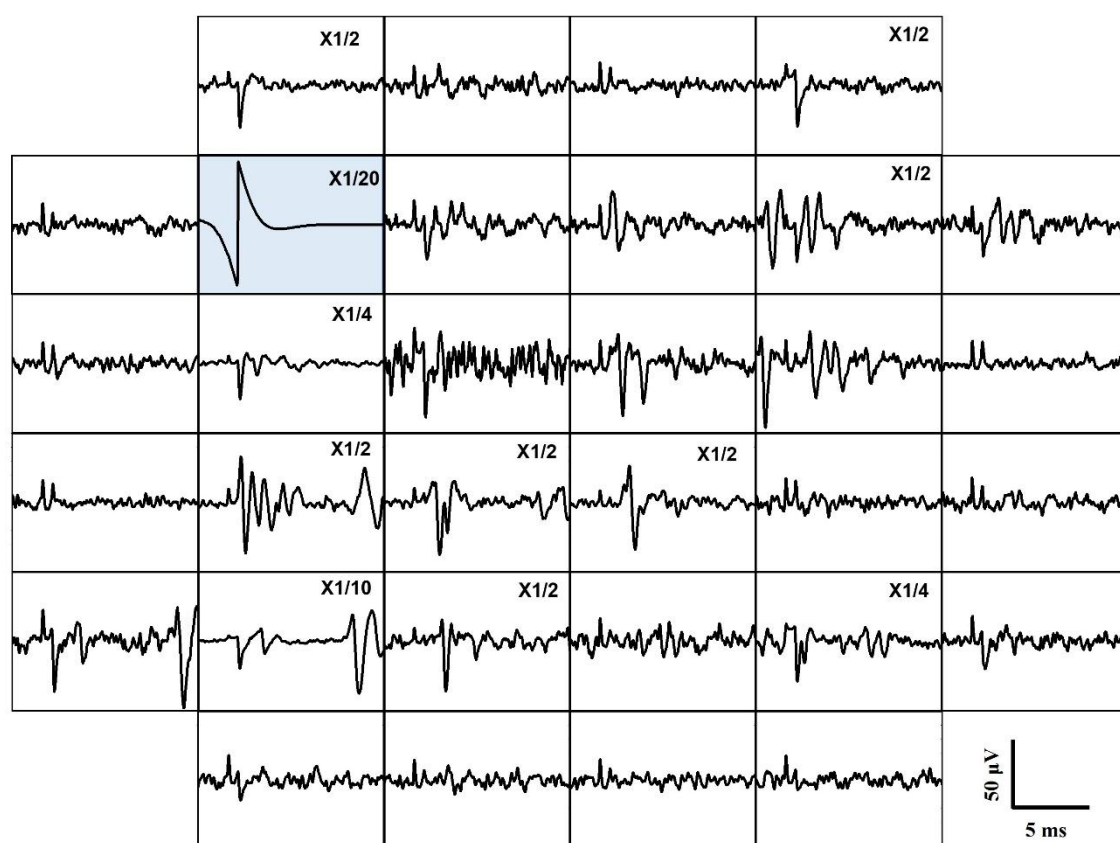


Fig. S6 Representative evoked signals recorded at all electrodes when V_{sp} was applied to E-11 (blue background) for 4CN

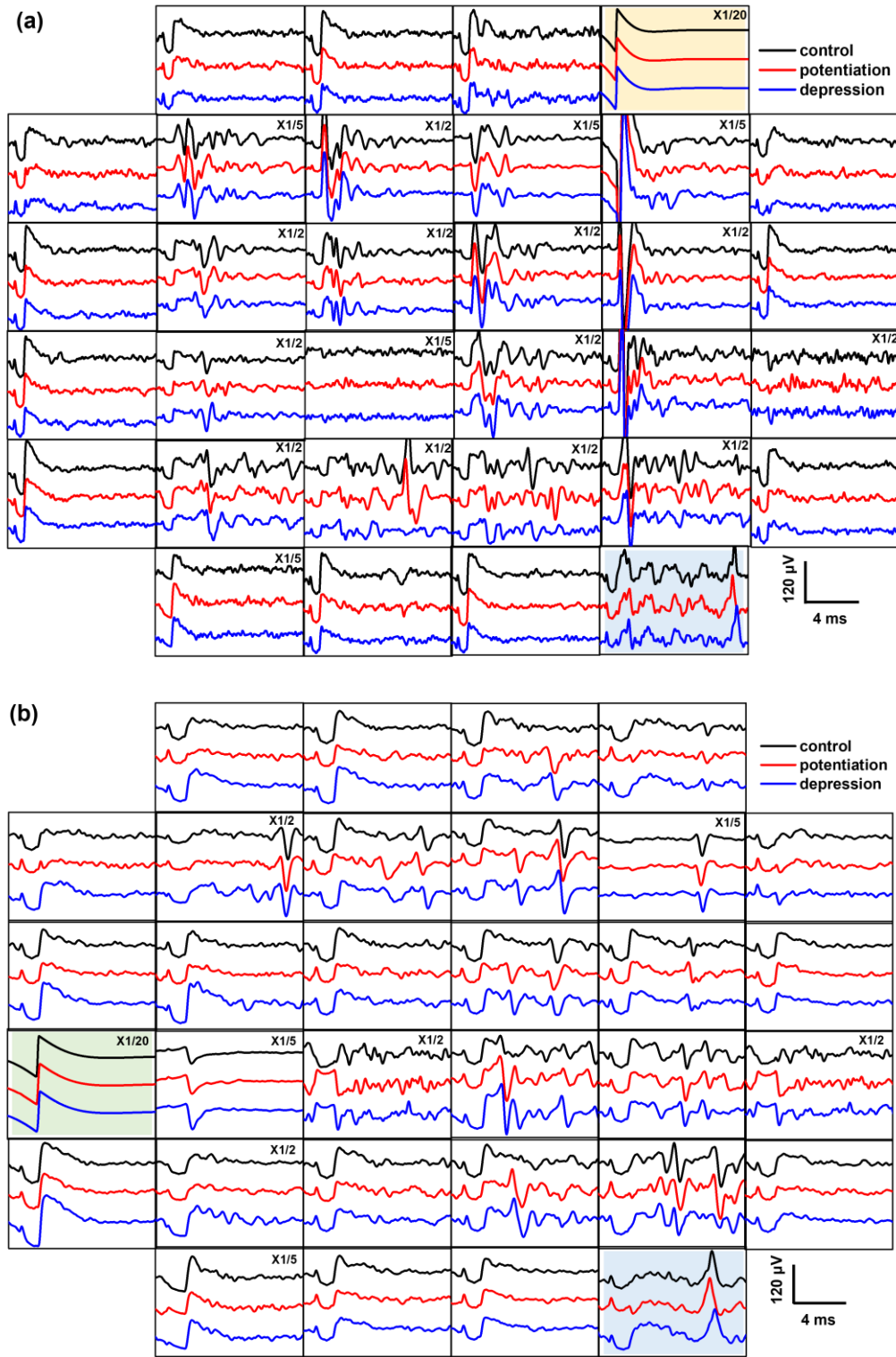
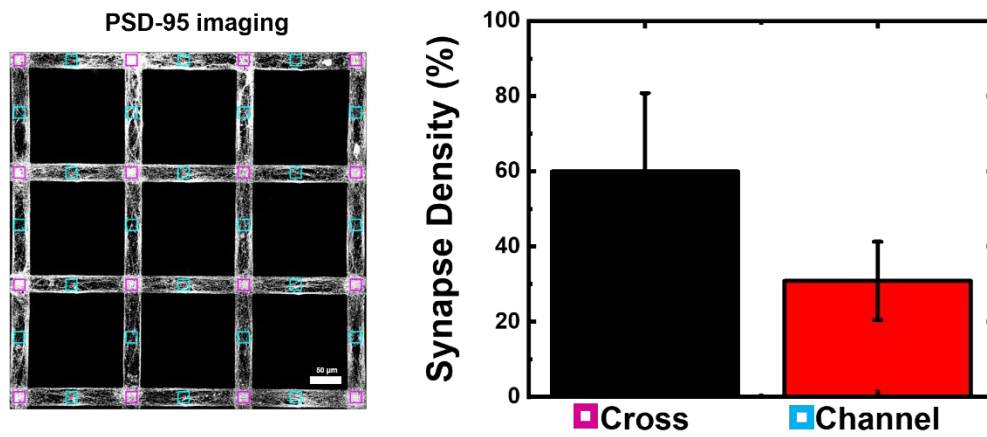


Fig. S7 (a) Evoked activities recorded from all electrodes upon the application of V_{sp} to (a) E-M (yellow background) and (b) E-C (green background) before potentiation (control, black), after potentiation (red), and after depression (blue) for 4CN. The potentiation and depression were induced by applying voltage pulse trains 1000 times at a frequency of 0.2 Hz to presynaptic neurons at (a) E-M (yellow background) or (b) E-C (green background), and postsynaptic neurons at E-H (blue background).

(a)



(b)

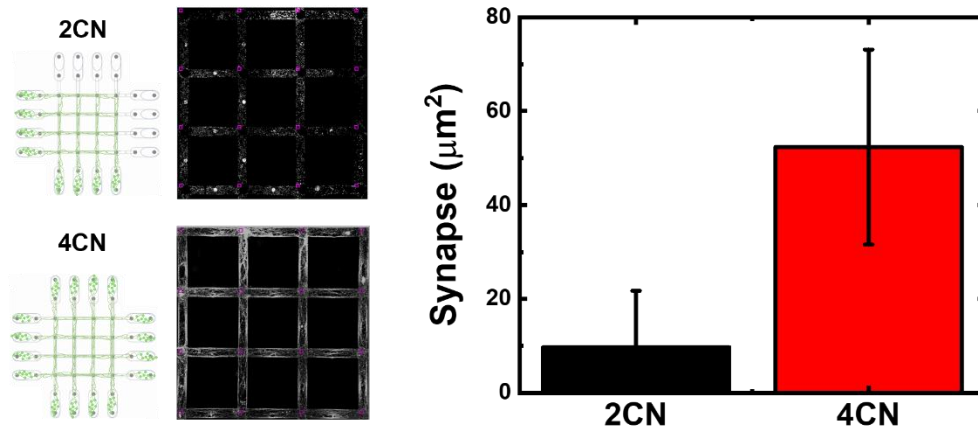


Fig. S8 (a) Synapse density in channel and cross regions. (b) Synapse density of 2CN and 4CN in cross regions. The fluorescent image on the left shows the PSD-95 stained data indicating synapses. The graph on the right presents the measured synapse density data. The magenta box region is designated as the cross region, and the cyan box region as the channel region, with analysis performed on these boxed areas.

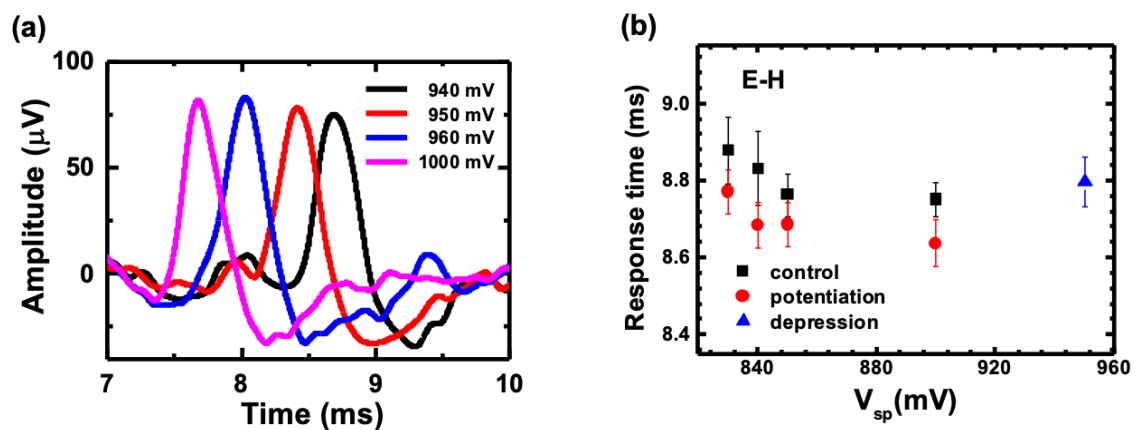


Fig. S9 (a) Representative evoked signals recorded at E-H when V_{sp} of various amplitudes was applied to E-M. (b) Response time of evoked signals as a function of V_{sp} for control (black), potentiation (red), and depression (green).

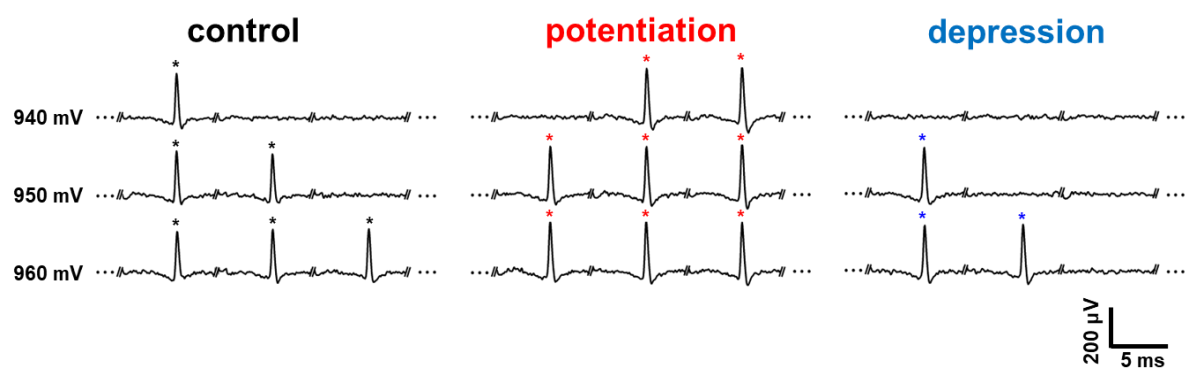


Fig. S10 Representative evoked signals recorded at E-H when V_{sp} of various amplitudes were repeatedly applied to E-C before potentiation (control), after potentiation, and after depression.

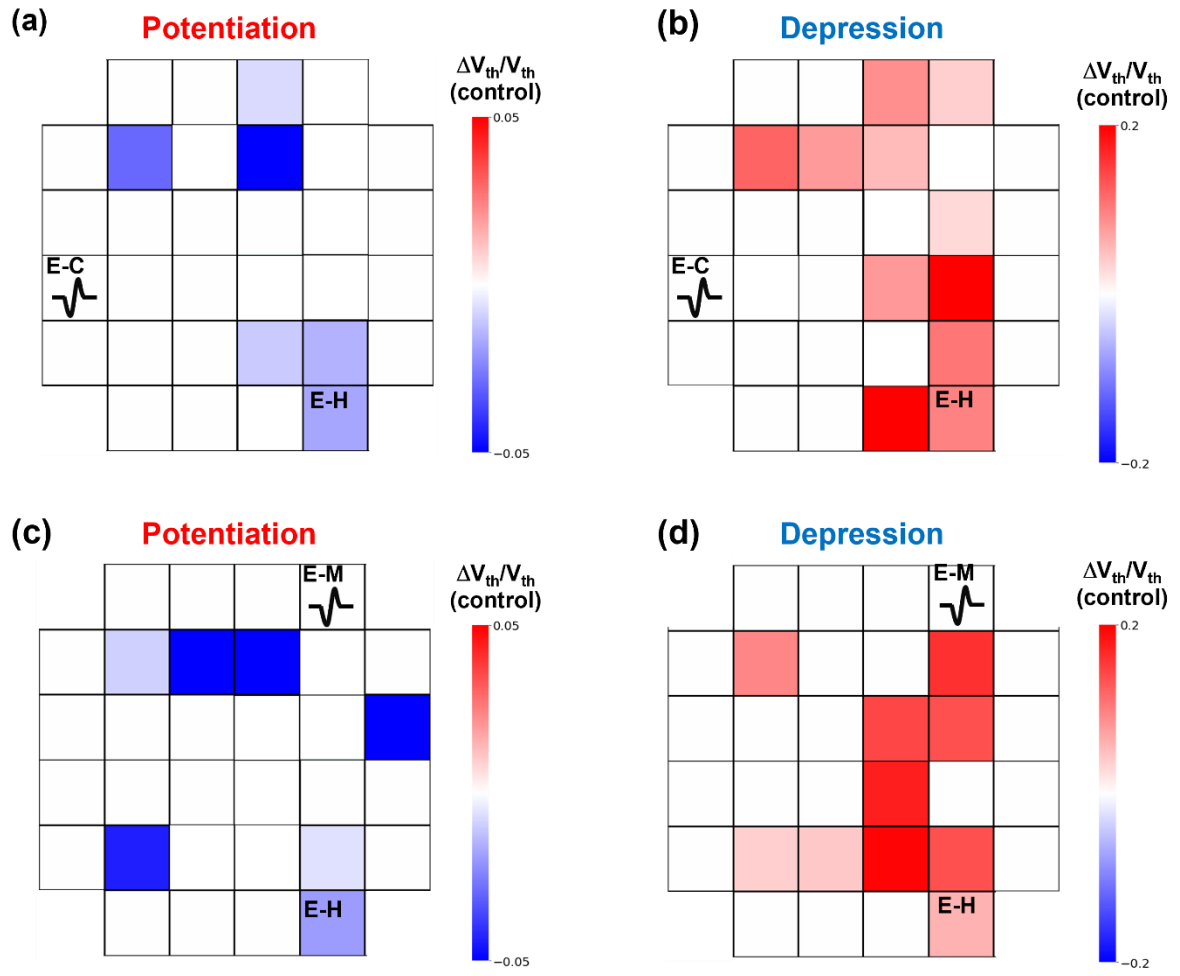


Fig. S11 $\Delta V_{th}/V_{th} = (V_{th} - V_{th(\text{control})})/V_{th(\text{control})}$ mapping after potentiation and depression induced using (a, b) E-C or (c, d) E-M as the presynaptic neuron and E-H as the postsynaptic neuron, respectively. V_{th} was estimated from the activation curves measured at E-H upon the application of V_{sp} of various amplitudes to (a, b) E-C or (c, d) E-M.

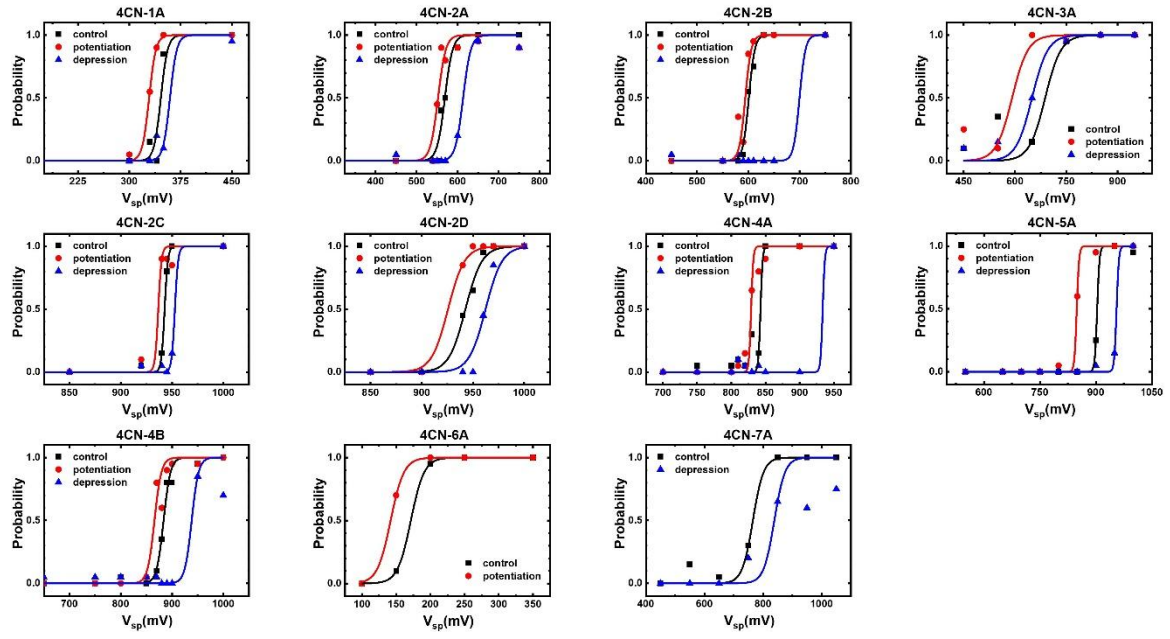


Fig. S12 Activation curves of different 4CNs. The probabilities of evoked spikes appearing at postsynaptic neurons were measured when V_{sp} of various amplitudes was applied to presynaptic neurons 20 times for control (black), potentiation (red), and depression (blue).

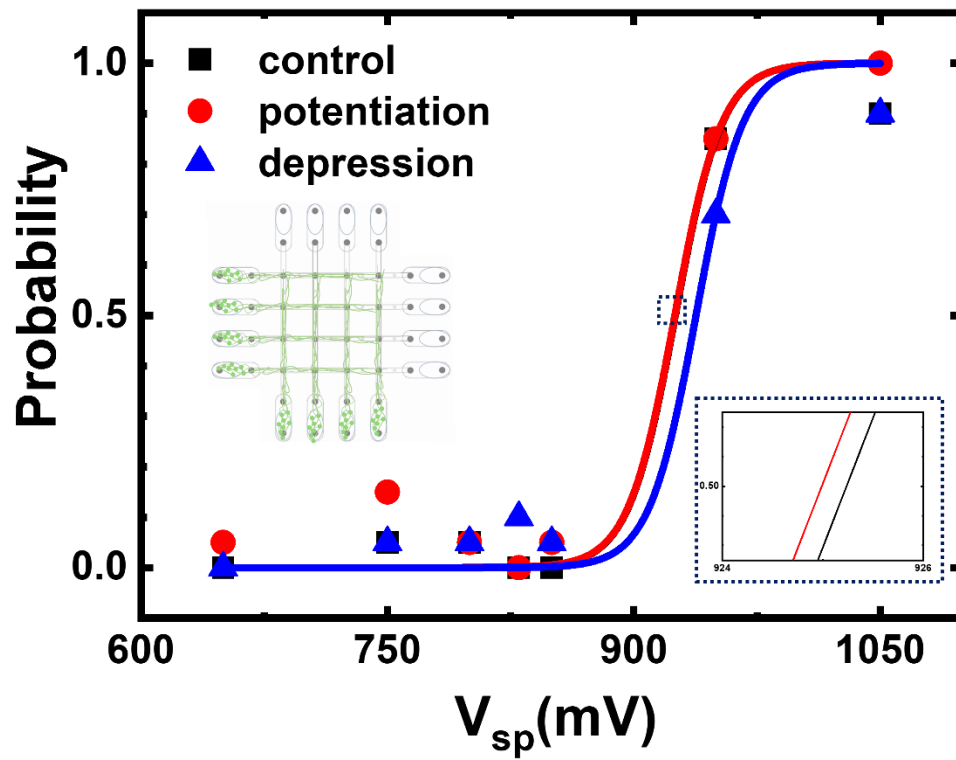


Fig. S13 Activation curve of 2CN. The probabilities of evoked spikes appearing at postsynaptic neurons were measured when V_{sp} of various amplitudes was applied to presynaptic neurons 20 times for control (black), potentiation (red), and depression (blue). The inset shows an enlarged plot indicated by the dotted box.

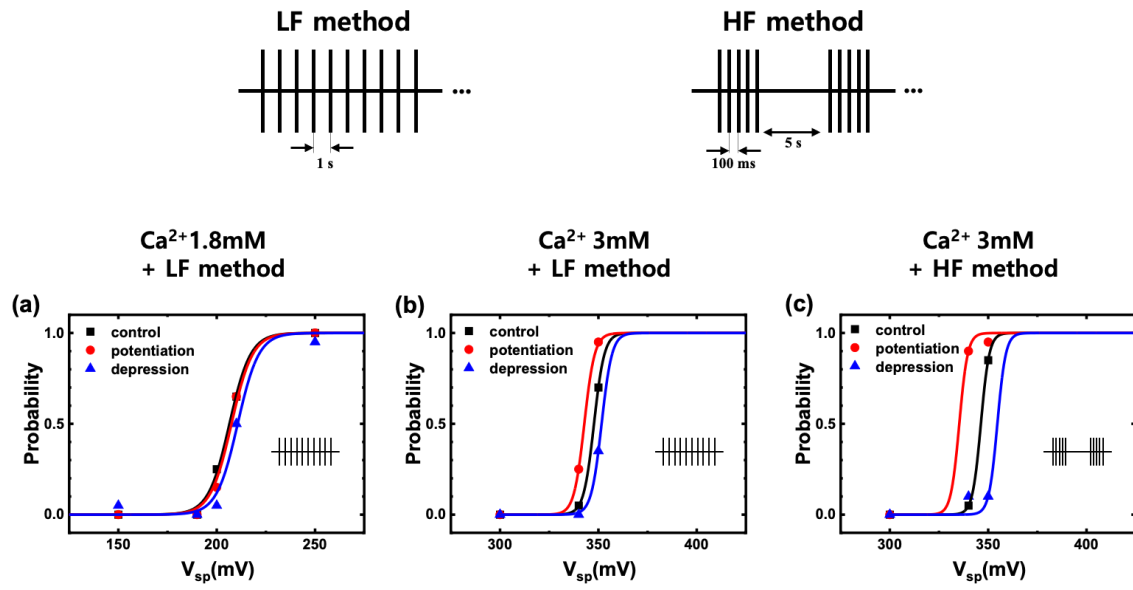


Fig. S14 Activation curves measured using (a) the 1.8 mM Ca²⁺ plus LF method, (b) the 3mM Ca²⁺ plus LF method, and (c) the 3mM Ca²⁺ plus LF method. The low frequency short- interval learning method (LF method) involves repeating single-pulse stimulation every second. The high frequency long-interval learning method (HF method) involves repeating a train of five pulses at 100ms intervals every five seconds.

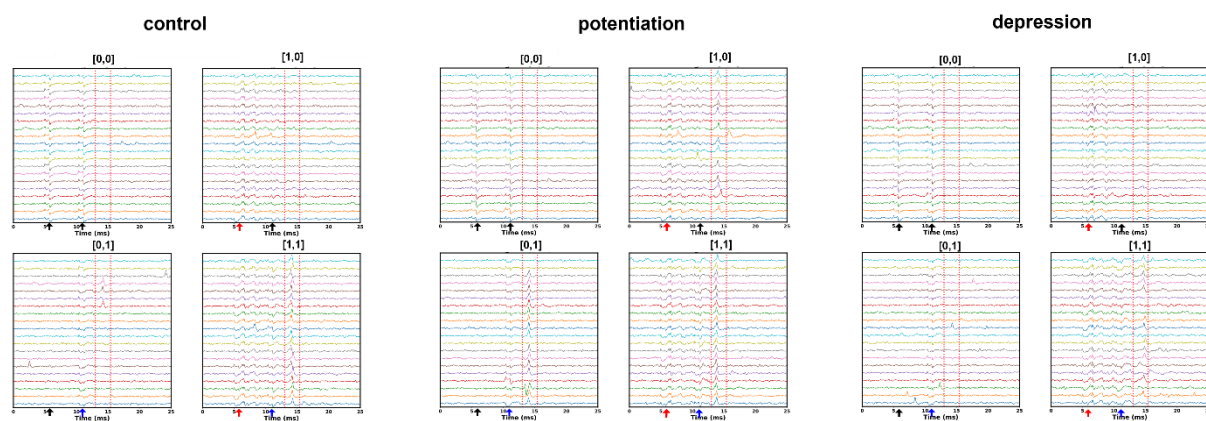


Fig. S15 Output signals were recorded at E-H when two input voltages of different amplitudes were applied 20 times to E-C and E-M before potentiation (control), after potentiation, and after depression. The first and second arrows indicate the time at which V_{sp} was applied to E-C and E-M, respectively. The black, red, and blue arrows represent V_{sp} values of 1, 840, and 870 mV respectively. The probability (P) of detecting evoked signal at E-H within the time window indicated by red dotted lines under different conditions is shown in Fig. 5A.

Table S1. Number of output spikes measured for different devices when two input voltages of different amplitudes were applied 20 times before potentiation (control), after potentiation, and after depression.

Device #	State	# of output spike			
		[0,0]	[1,0]	[0,1]	[1,1]
Device 1	control	0	0	4	18
	potentiation	0	11	17	20
	depression	0	0	1	17
Device 2	control	0	2	0	18
	potentiation	0	15	13	20
	depression	0	0	0	14
Device 3	control	0	1	2	12
	potentiation	0	13	13	15
	depression	0	0	2	8
Device 4	control	0	1	0	16
	potentiation	2	15	15	20
Device 5	control	0	0	9	15
	potentiation	0	10	17	19
	depression	0	0	0	13
Device 6	control	0	3	2	18
	potentiation	0	20	15	20
	depression	0	0	0	14
Device 7	control	0	3	4	20
	potentiation	0	18	13	20
	depression	0	1	1	16
Device 8	control	0	3	2	19
	potentiation	0	16	13	20
	depression	0	1	1	13
Device 9	control	0	0	3	18
	potentiation	0	13	20	20
	depression	0	0	0	14

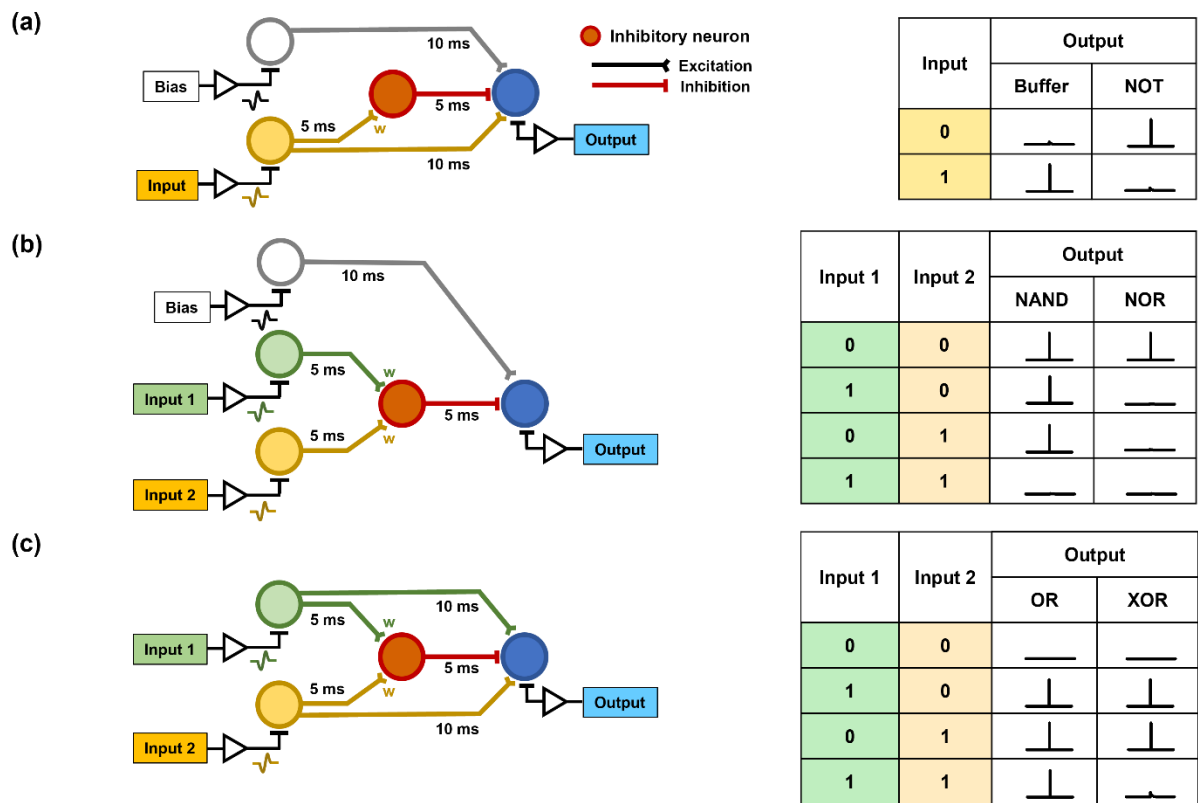


Fig. S16 (a) Buffer/NOT, (b) NAND/NOR, and (c) OR/XOR logic gates simulated using the neural networks consisting of excitatory and inhibitory neurons.

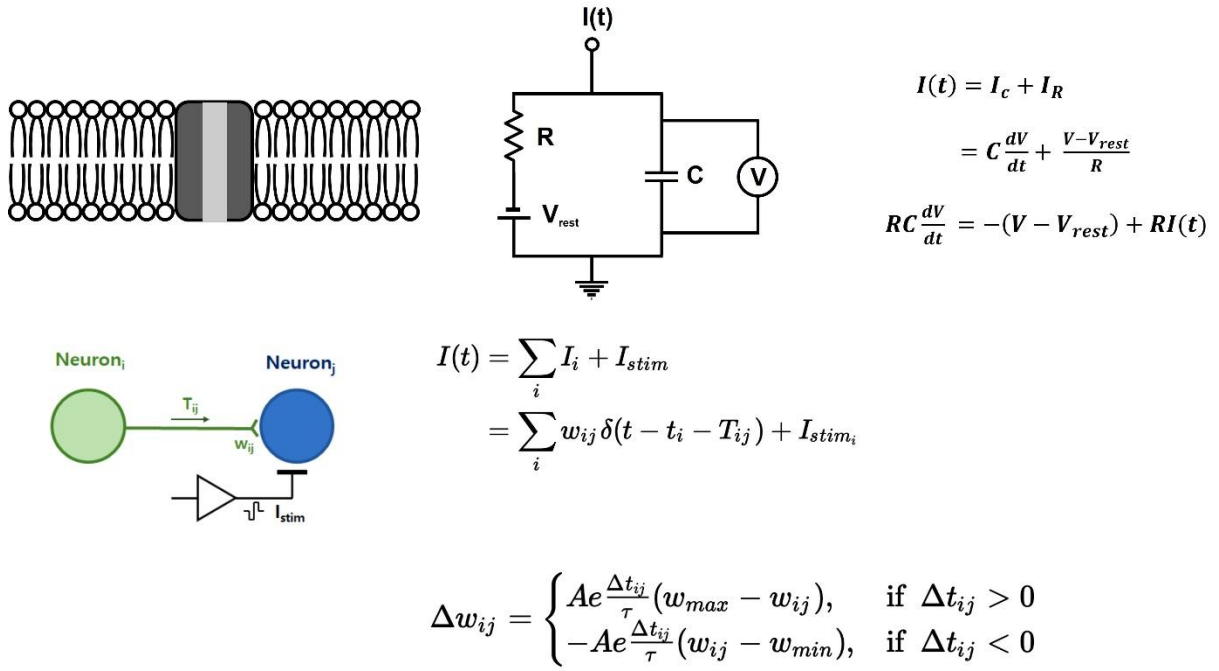


Fig. S17 Model of a leaky integrate-and-fire neuron, the current received by neurons with an external stimulus, and synaptic strength modulation due to spike-timing-dependent plasticity (STDP).